JOURNAL OF CATALYSIS **166,** 98–107 (1997)
ARTICLE NO. CA971498

A Temperature-Programmed and Transient Kinetic Study of CO_2 Activation and Methanation over CeO_2 Supported Noble Metals

Carla de Leitenburg,* Alessandro Trovarelli,* and Jan Kašpar†

Dipartimento di Scienze e Tecnologie Chimiche, via Cotonificio 108, Università di Udine, 33100 Udine, Italy; †Dipartimento di Scienze Chimiche, via Giorgieri 1, Università di Trieste, 34127 Trieste, Italy

Received June 24, 1996; revised October 17, 1996; accepted October 17, 1996

The interaction of CO_2 with noble metals deposited on ceria surfaces have been studied by temperature-programmed techniques. A transient kinetic study of CO_2 activation and methanation over M/CeO_2 has also been conducted. The mechanism of interaction between M/CeO_2 and CO_2 and its activation in the presence of H_2 to CH_4 is strongly influenced by the reduction temperature, regardless of the metal employed. It is suggested that, by increasing the reduction temperature, a progressive reduction of bulk CeO_2 takes place, which is not promoted by the presence of the metal. The interaction mechanism suggested involves activation of CO_2 on a surface Ce^{3+} site with formation of CO followed by oxidation of Ce^{3+} to Ce^{4+}. The presence of oxygen bulk vacancies will create the additional driving force for the reduction of CO_2 to CO and/or surface carbonaceous species which then rapidly hydrogenate to CH_4 over the supported metal.

INTRODUCTION

Materials containing CeO_2 have been frequently investigated in recent years owing to the use of CeO_2 as an effective component in three-way catalysts for automotive exhaust control (1). Ceria has been used as a support for precious metal catalysts in many applications, from CO/NO reaction (2) to CO and CO_2 hydrogenation (3) and CO oxidation (4). Although the detailed mechanism is still unknown, it is clear that the role of ceria in promoting these reactions lies in its ability to create surface and bulk vacancies and in the effectiveness of its Ce(III)/Ce(IV) redox couple (5). The role of the noble metal during reduction should be that of providing a reservoir of reducing H species through the well-known spillover effect, hence increasing the ability of CeO_2 to form vacancies and to act as an effective oxygen storage/release component for redox catalysis. Therefore, the nature of the interaction between ceria and noble metals in a reducing atmosphere is different from that observed on other well-known reducible supports such as TiO_2 or Nb_2O_5 (6–9). Evidence of this difference is also found in the catalytic properties of noble metals supported on ceria and titania; while, for example, a reducing treatment at 773 K suppresses the rate of CO_2 hydrogenation on Rh/TiO_2 or Rh/Nb_2O_5, it results in a strong temporary enhancement of reactivity over Rh/CeO_2 (9). The presence of oxygen vacancies on CeO_2, located both on the surface and in the bulk, are believed to be the driving force leading to this behaviour.

As part of a more general investigation of CO_2 activation on metals supported on reducible oxides, we studied here CO_2 decomposition and methanation over noble metals supported on CeO_2. Temperature-programmed reduction (TPR), decomposition (TPD), and surface reaction (TPSR) have been used to better elucidate the role of ceria in CO_2 activation, while catalytic studies were carried out under both pulse and steady-state conditions. The aim of this paper is to elucidate the role played by the metal and the support in CO_2 activation over M/CeO_2 (M = Pd, Pt, Rh, Ir, and Ru) subjected to different reducing treatments under hydrogen and, in particular, to find some common features in the behaviour of the different metals.

EXPERIMENTAL

Catalyst Preparation

Cerium oxide (19 m^2/g B.E.T. area) was prepared by hydrolysis of cerium nitrate with NH_4OH followed by drying and calcination at 823 K. Noble metal catalysts (nominal loading 1 wt%) were prepared by incipient wetness of CeO_2 with an aqueous solution of the appropriate metal salts ($RhCl_3$, $Rh(NO_3)_3$, $RuCl_3$, H_2PtCl_6, $PdCl_2$, $IrCl_3$). They were then dried at 373 K overnight and calcined in air at 773 K for 2 h. Reduction was carried out under H_2 flow (60 ml min^{-1}) at 473 K (LTR) or at 773 K (HTR) for 2 h.

Hydrogen Chemisorption and Temperature-Programmed Reduction (TPR)

H_2 adsorption was measured at 298 K after LTR and HTR. After reduction the samples were evacuated at 573 K (10^{-5} torr) for 2 h. The H_2 uptake was calculated by extrapolating the linear part of the adsorption isotherm to zero pressure. A Sorptomatic 1990 Carlo Erba instrument, interfaced to a computer, was used. The experimental procedure

0021-9517/97 $25.00

and the apparatus for TPR analysis were described in a preceding paper (3). Briefly, the sample was heated in a U-shaped conventional quartz micro reactor from 300 to 1450 K (heating rate 10 K min^{-1}) in a flowing hydrogen/argon mixture (30 ml min^{-1}, 5.22% H_2 in Ar); the hydrogen consumption was monitored using a thermal conductivity detector. The quantitative evaluation of H_2 consumed was done by calibrating the apparatus with the reduction of CuO to metallic copper.

Temperature-Programmed Desorption (TPD) and Temperature-Programmed Surface Reactions (TPSR)

The experiments were performed using the apparatus described in a recent paper (10). The catalyst (200 mg) was loaded in a quartz micro reactor and oxygen was removed in flowing He (10 ml min^{-1}) at 800 K for 1 h. Before reduction and prior to CO_2 adsorption, the catalyst was further treated in helium at 573 K for 1 h. The adsorption was performed at 298 K by pulsing three consecutive injections (4.1 μmoles) of CO_2. Excess CO_2 was removed in flowing helium until no further desorption of CO_2 could be detected (60 min approx.). The catalyst was then ramped at a linear heating rate of 25 K min^{-1} in flowing He (50 ml min^{-1}). The TPD experiments were performed following CO_2 adsorption after LTR (run TPD1), after HTR (run TPD2) and after run TPD2 without intermediate reduction (run TPD3). The desorbing gases were analyzed by a quadrupole mass spectrometer (VG 200 instrument). The observed intensity for CO_2 and CO were normalized with respect to a standard mixture of the same range of concentration for both TPD and TPSR experiments in order to account for CO_2 dissociation into the ion source.

TPSR was performed in the same apparatus described for TPD, and the samples were pretreated under the same conditions. After saturation with pulses of CO_2, the catalysts were heated from 300 to 900 K (heating rate 25 K min^{-1}) in 8% H_2 in He.

Catalytic Studies

Catalytic studies were carried out under both steady-state and transient (pulse) conditions. Before the experiments, the catalysts were reduced in H_2 (60 ml min^{-1}) at 500 K (LTR) or 773 K (HTR) for 2 h. Pulse experiments were performed according to the method described by Mori (11). A known amount of CO_2 (0.81 μmoles) was injected into the catalyst bed, into an H_2 stream (30 ml min^{-1}), by using a six-way valve. CO_2 was adsorbed on the catalyst bed and then hydrogenated selectively to CH_4 and H_2O. The two products were separated in a short Porapak Q column inserted between the reactor and the detectors. At the end of the column, a splitter enabled simultaneous detection of CH_4 and H_2O on a flame ionization detector (FID) and on a thermal conductivity detector (TCD), respectively. When the rate of formation of methane was measured, the Porapak Q column was excluded in order to decrease the dead volume from the reactor to the detector and thus avoid the dispersion of CH_4. Since H_2O is not detected by FID, the FID response is directly related to the rate of CH_4 formation (11). The detector response factor was determined by injecting known amounts of CH_4 into the system.

Catalytic tests under steady-state conditions were carried out by using a conventional flow micro reactor in the differential mode. The conditions were as follows: GHSV 6000 h^{-1}, $CO_2/H_2 = 1/4$, reaction temperature 500–550 K. Reaction products were analyzed by an on line HP5890 Gaschromatograph equipped with a Porapak Q column and TCD and FID detectors. Unless otherwise specified, we avoided the use of turnover frequencies (TN) owing to the uncertainties of H_2 uptake on CeO_2.

A series of additional experiments in continuous conditions were conducted by using a diluted mixture (CO_2 (2%)/H_2 (5.95%)/He (92.05%)). The amount of catalyst used was in the range 80–150 mg and the space velocities were 7500–10000 h^{-1}. Methane evolved was directly and continually monitored with a FID; under such conditions the time delay between introduction of the reagents and monitoring of the products was less than 15 s, thus allowing the measurement of the initial rate over the virgin catalyst (9). The system was calibrated by using CH_4/He mixtures of known CH_4 concentration. Temperature-programmed methanation of carbon was carried out on samples treated for 35 min under these reaction conditions. After reaction the samples were cooled to room temperature in He and then ramped (10 K min^{-1}) under H_2 (30 ml min^{-1}) from 300 to 800 K.

RESULTS

Hydrogen Chemisorption and Temperature-Programmed Reduction

Hydrogen chemisorption after LTR and HTR for all metal-supported samples is reported in Table 1. High H/M values are obtained after reduction at 473 K; in the case of Ir

TABLE 1

Hydrogen Chemisorption after Low and High Temperature Reduction[a]

	H/M	
Sample	LTR	HTR
Rh/CeO_2	0.93	0.61
Ir/CeO_2	2.97	0.79
Ru/CeO_2	0.98	0.57
Pt/CeO_2	1.26	0.23
Pd/CeO_2	0.63	0.27

[a] LTR = reduction at 473 K, HTR = reduction at 773 K.

and Pt, H/M values greater than 1 are observed. These high values for H_2 uptake are typical of CeO_2-supported catalysts and are a consequence of the high H_2 spillover rate (12, 13). An examination of the data reported in Table 1 reveals a partial suppression of H_2 uptake after the HTR. Low H/M values were observed, especially for Pd and Pt; however, it should be noted that, despite a relatively high H/Ir after the HTR, there is also a significant decrease in the H_2 uptake by Ir, since a ratio of the LTR/HTR uptakes of 3.8 is obtained.

Temperature-programmed reduction profiles of all samples are reported in Fig. 1. For pure CeO_2 two peaks were observed at around 835 and 1090 K, characteristic of reduction of surface and bulk ceria; the degree of reduction to Ce^{3+}, as estimated by integrating the area of the curve, is approximately 46% at 1450 K, corresponding to $CeO_{1.77}$. This is in agreement with reported data for reduction of CeO_2 at these temperatures (14). The presence of the noble metal strongly modifies the features of the TPR traces. The first peak almost disappears, while a strong signal appears at around 350–500 K and was assigned to the reduction of the metal (15, 16). A quantitative estimation of these low temperature signals indicates that the amount of H_2 consumed greatly exceeds that required for the reduction of the metal oxides as calculated according to the reduction of Rh_2O_3, RuO_2, IrO_2, PtO_2, and PdO to the corresponding metal. This fact, together with an almost complete disappearance of the low temperature peak at 835 K, which is present in CeO_2 only, indicates that most of H_2 consumed in the low temperature region is used to remove the readily available surface oxygen through the spillover mechanism, as already observed with Rh (12), Ir (17), and Pd (13). By subtracting the TPR trace of M/CeO_2 from that of the corresponding M/SiO_2, in which H_2 consumption can be related to complete reduction of the metal only, it is possible to quantify the extent of reduction of CeO_2 in the presence of the metal, assuming that all of the extra hydrogen consumed is used for CeO_2 reduction. This is shown in Fig. 2 for CeO_2 and Ru/CeO_2 and detailed in Table 2 for all the examined

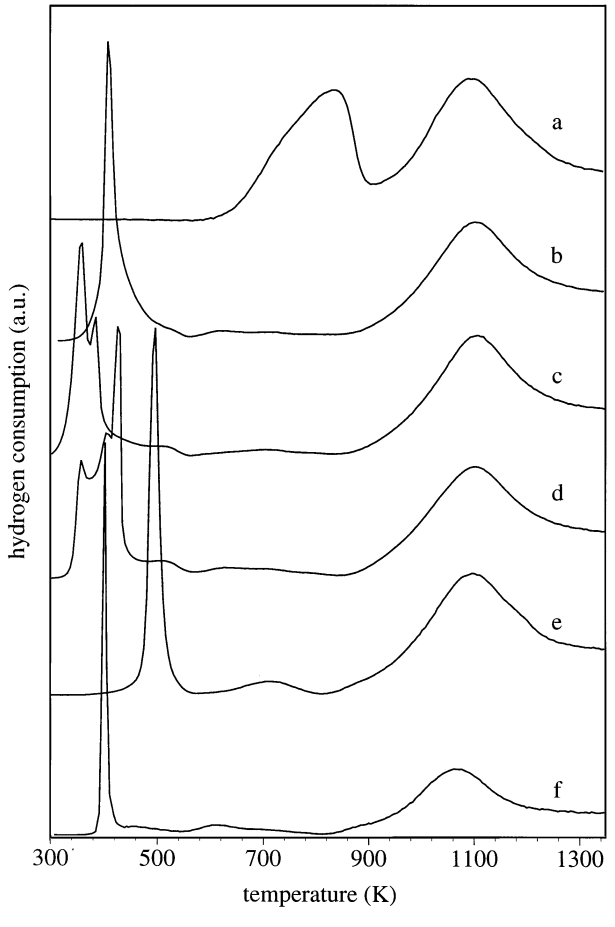

FIG. 1. Temperature-programmed reduction profiles of (a) CeO_2; (b) Rh/CeO_2; (c) Ir/CeO_2; (d) Ru/CeO_2; (e) Pt/CeO_2; (f) Pd/CeO_2.

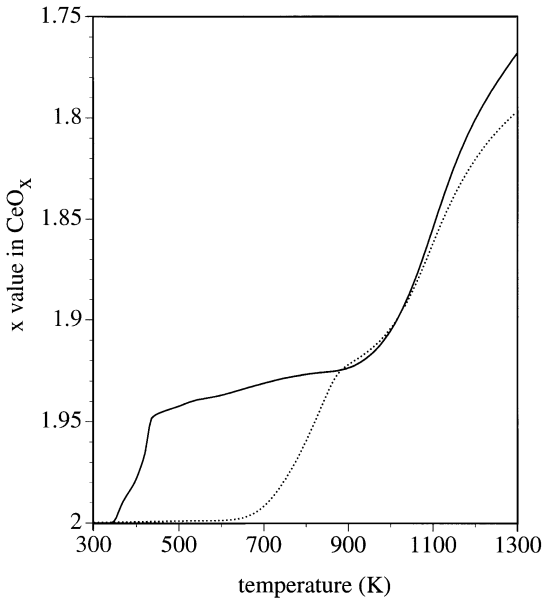

FIG. 2. Extent of CeO_2 reduction in CeO_2 (····) and Ru/CeO_2 (—) as calculated from TPR measurements.

TABLE 2

Degree of Reduction of the Support and Peak Temperatures as Determined from TPR

Sample	Degree of reduction CeO_x[a] 500 K	800 K	1450 K	Peak Temperature K
CeO_2	2.00	1.96	1.77	835, 1090
Rh/CeO_2	1.95	1.94	1.73	408, 619, 1100
Ir/CeO_2	1.97	1.95	1.76	357, 385, 705, 1110
Ru/CeO_2	1.95	1.93	1.73	358, 425, 630, 1105
Pt/CeO_2	1.96	1.95	1.74	495, 715, 1100
Pd/CeO_2	1.96	1.93	1.73	405, 605, 1062

[a] Degree of support reduction expressed as CeO_x. Standard deviation $x = \pm 0.01$.

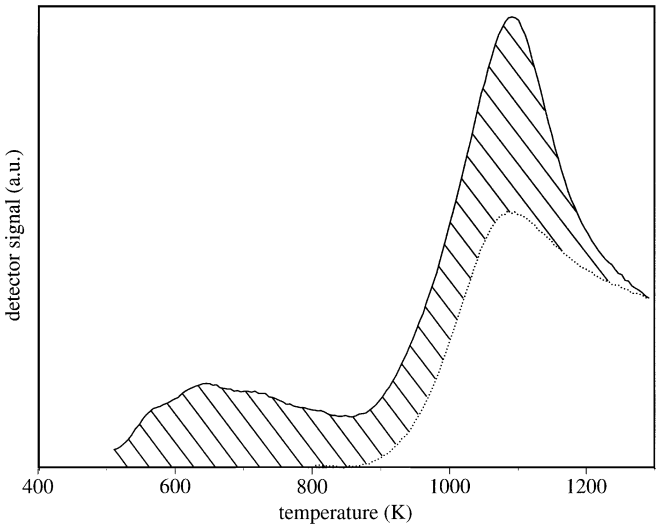

FIG. 3. TPR of Ru/CeO_2 after reduction for 2 h at 473 K (—) and 773 K (···). The shaded area represents the difference between the two curves.

samples. It is clearly shown that reduction of CeO_2 in the presence of the metal is greatly increased, especially in the low and medium temperature regions (350 K < T < 800 K), where reduction of the more readily available surface and near surface Ce(IV) is observed. The TPR curves for metal-supported samples can be divided into three parts: (1) the region between 350 and 500 K in which reduction of ceria by a spillover mechanism takes place; at these temperatures a reduction of approximately 10% is reached, corresponding to a stoichiometry for CeO_x with $x = 1.95-1.97$; no reduction over pure ceria is observed in this region; (2) in the second portion of the curve, from ca 500 to 800 K, reduction under TPR conditions increases very slowly; compare Table 2; (3) in the high temperature range (900–1300 K) a further increase in the reduction rate is observed for all samples, reaching values close to $x = 1.75$. The overall degree of reduction is only slightly affected by the presence of the metal; a degree of reduction ranging from 46 to 54% is observed for CeO_2 in all the metal-supported samples. Moreover, with some metals, a splitting of the low temperature signal is observed, which might be due to a less homogeneous deposition of metal crystallites of different crystal sizes (18).

To estimate the degree of reduction after LTR and HTR a Ru/CeO_2 catalyst was subjected to these treatments followed by TPR analysis. The results, reported in Fig. 3, indicate that there is a significant difference in the degree of reduction of the support as indicated by the shaded area. Under assumption that the final degree of reduction of CeO_x in the Ru/CeO_2 sample is constant at $x = 1.73$ (Table 2), we estimated a value of $x = 1.94$ and $x = 1.87$ after LTR and HTR, respectively.

Temperature-Programmed Desorption and Decomposition of CO_2 on M/CeO_2

The sequence of Fig. 4 shows the traces of CO and CO_2 desorbing from Pt/CeO_2 following CO_2 adsorption after LTR and HTR. There are significant differences in the behaviour of the catalyst subjected to different reduction treatments; after reduction at 473 K there is a broad desorption of CO_2 with a shoulder at around 400 K. A small amount of CO was detected in this experiment. By increasing the reduction temperature to 773 K the situation changed. The presence of both CO and CO_2 is detected, and the total amount of desorbed CO exceeds that of CO_2. A third TPD run was performed after adsorbing CO_2 on the samples obtained from the second TPD experiment. The situation is partially reversed, since a strong increase in CO_2 evolution is observed. Similar profiles were obtained with the other metal catalysts, and the data are summarized in Table 3. After LTR the CO_2/CO ratio observed for pure ceria is significantly higher than those observed over the metal-loaded samples. In contrast, similar values were observed for all samples after HTR, indicating the important role of ceria in CO_2 activation in this case. In agreement with what is depicted in Fig. 4, an increase in the CO_2/CO ratio during TPD3 was observed, in contrast to TPD2. In summary, it appears that, as a general trend, mainly CO_2 is desorbed after a low temperature reduction, while after a high temperature reduction CO_2 is mainly decomposed to

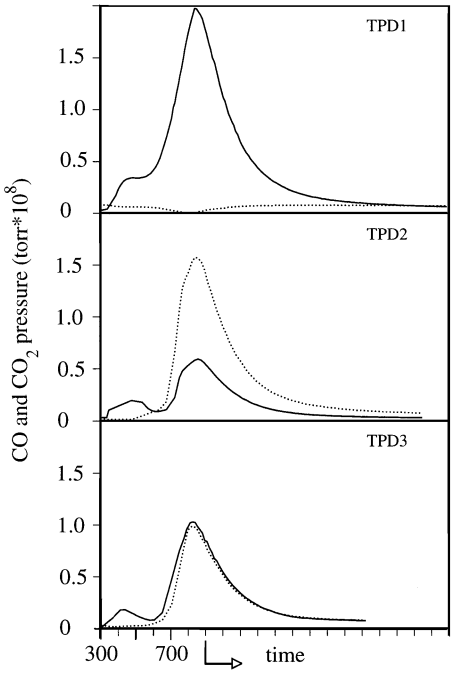

FIG. 4. Temperature-programmed desorption of CO (···) and CO_2 (—) from Pt/CeO_2 following CO_2 adsorption after LTR (TPD1), HTR (TPD2) and after TPD2 (TPD3).

TABLE 3

Temperature-Programmed Desorption (TPD) of Adsorbed CO_2 from M/CeO_2 Catalysts: Relative CO_2/CO Amounts Evolved

Sample	TPD1[a] CO_2/CO	TPD2[b] CO_2/CO	TPD3[c] CO_2/CO
Rh/CeO_2	10(±1)[d]	3.3(±0.5)	9.6(±1)
Ru/CeO_2	24(±3)	1.1(±0.1)	17(±2)
Pt/CeO_2	28(±4)	0.4(±0.06)	1.1(±0.1)
Pd/CeO_2	33(±5)	0.7(±0.1)	—
Ir/CeO_2	28(±4)	1.6(±0.2)	16(±2)
CeO_2	56(±8)	0.56(±0.08)	5.2(±0.7)

[a] TPD of adsorbed CO_2 after LTR.
[b] TPD of adsorbed CO_2 after HTR.
[c] TPD of adsorbed CO_2 after TPD2.
[d] The error is reported in brackets.

give a substantial desorption of CO, indicating a possible activation of CO_2 by the support.

Temperature-Programmed Surface Reaction

Figure 5 shows the TPSR profile of methane formation from M/CeO_2 after a low and a high temperature reduction. Traces of C_2 and C_3 hydrocarbons were also observed; however, their concentrations are lower by two orders of magnitude as compared to CH_4. After LTR, with the exception of Ru/CeO_2, a single peak located at 550–750 K is observed. The HTR modifies the reaction profile, since either a shoulder at lower temperatures appears and/or the peak temperature shifts to lower values. This is particularly evident in the case of Pt, in which a difference of more than 200 K is observed between the two maxima. For all catalysts tested, the onset of CH_4 formation after HTR is observed to be several degrees lower than that of LTR. In the case of Rh/CeO_2, the samples were subjected to HTR by varying the reduction times and increasing the reduction temperature to 873 K. The resulting TPSR profiles are reported in Fig. 6. It is shown that, by increasing HTR reduction times from 2 to 4 h and the reduction temperature from 773 K to 873 K, the CH_4 formation rate significantly increases at low temperature as indicated by the tailing of the peaks in Fig. 6. No CH_4 evolution is observed after LTR and HTR on pure ceria.

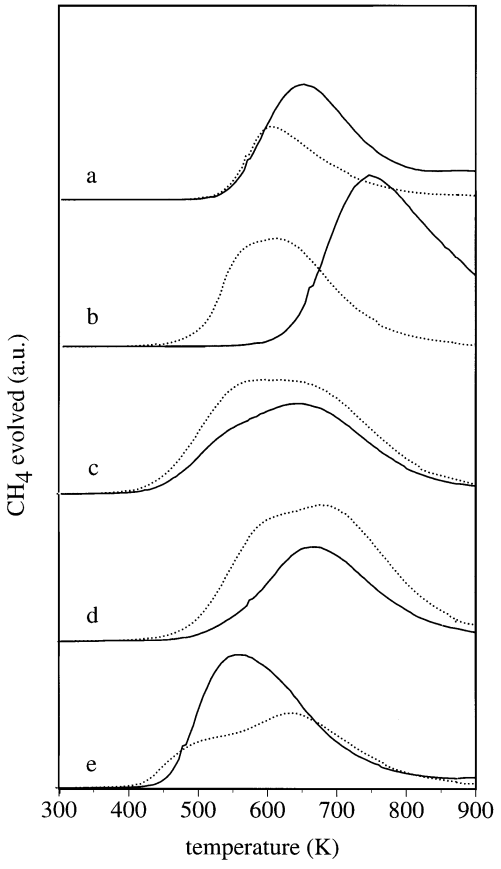

FIG. 5. Temperature-programmed surface methanation of CO_2 adsorbed after LTR (—) and after HTR (···). (a) Pd/CeO_2; (b) Pt/CeO_2; (c) Ru/CeO_2; (d) Rh/CeO_2; (e) Ir/CeO_2.

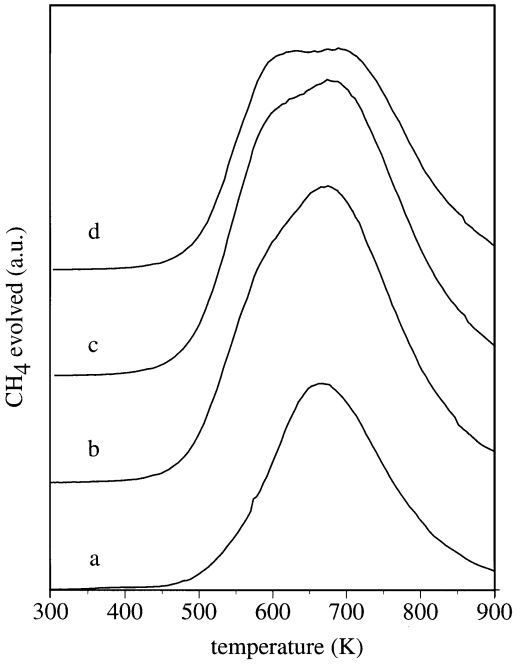

FIG. 6. Temperature-programmed surface methanation of adsorbed CO_2 on Rh/CeO_2 catalyst after LTR (a) and after 2 (b) and 4 (c) hours of reduction at 773 K, and 1 h at 873 K (d).

CO_2 Methanation under Continuous and Transient Conditions

The effect of varying the reduction temperature was also investigated in CO_2 hydrogenation under both steady-state and transient pulse conditions. Steady-state activities are reported in Table 4, together with reaction conditions. According to these results the catalyst can be divided into two

TABLE 4

Steady-State Activity for CO_2 Hydrogenation over CeO_2-Supported Catalysts[a]

	LTR		HTR	
	rCO	rCH$_4$	rCO	rCH$_4$
Ir	2160	167	1000	39
Pd	2348	256	1415	76
Pt	6220	26	4527	6
Rh	—	2210	—	1520
Ru	—	3292	—	1550

[a] Reaction conditions: $T = 550$ K (Ir, Pd, Pt) 500 K (Rh, Ru); $CO_2/H_2 = 1/4$; weight of catalyst 0.1–0.2 g, total flow 15 ml min^{-1}. Rate: μmole $* g_{cat.}^{-1} * h^{-1}$.

groups: Ru and Rh which give CH_4 only as the reaction product and Pt, Pd, and Ir which give both CO and CH_4. The effect of reduction temperature does not greatly modify behaviour; a general decrease in activity is observed by increasing the temperature of the reduction treatment, which can be related to a decrease in exposed metal sites, as detected by H_2 chemisorption.

Under pulse conditions CH_4 and H_2O are the only reaction products in the case of Rh and Ru, while in the case of Pt, Pd, and Ir a small quantity of CO is also formed after LTR. The CH_4 elution peak was analyzed by using the pulse surface reaction rate analysis (PSRRA) method described by Mori *et al.* (11). Typical results are reported in Fig. 7 for Ru/CeO_2. The rate of methane formation gradually decreases with time from the top of the curve for the LTR catalyst, while a more intense peak with a sharp decrease is observed for the catalyst reduced at 773 K. A linear relationship, corresponding to a first-order kinetic, was found to hold for all catalysts tested. Reaction rates were calculated at initial conditions by using the intercept of the linear plot at time $t = 0$ for all catalysts after LTR and HTR.

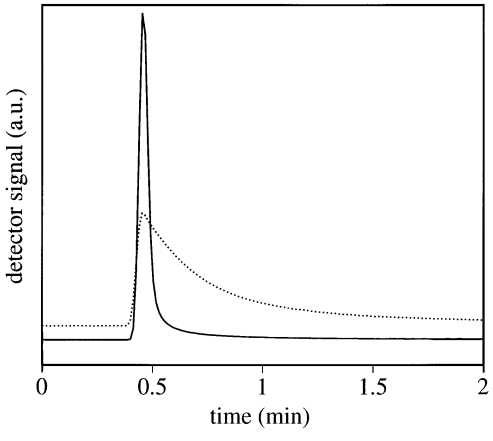

FIG. 7. FID response for CH_4 formed following the CO_2 pulse in flowing H_2 after LTR (····) and HTR (——) on a Ru/CeO_2 catalyst.

TABLE 5

Kinetic Parameters for CH_4 Formation in $CO_2 + H_2$ Reaction under Transient-Pulse Conditions[a]

	LTR		HTR		
	k^b	r^c	k	r	r'
Ir	0.0042	340	0.334	4120	1720
Pd	0.0073	880	0.126	1080	780
Pt	0.014	2400	0.514	27850	1000
Rh	0.055	19940	0.445	101100	12940
Ru	0.054	12820	0.651	152790	12830

[a] Reaction conditions: $T = 550$ K (Pt) 500 K (Ir, Pd, Rh, Ru); CO_2 pulse size 20 μl; Cat. weight 20 mg; carrier flow 30 ml H_2 min^{-1}.

[b] k: rate constant, (s^{-1}).

[c] r: rate calculated during the first CO_2 pulse, μmole $* g_{cat.}^{-1} * h^{-1}$; r': rate calculated after 10 pulses.

As shown in Table 5, k and reaction rates are considerably larger after HTR than after LTR. HTR induces an increase up to one order of magnitude in the reaction rate after the first pulse; this enhancement is much more evident with Ru, Rh, and Pt and less marked for Pd and Ir. However, during successive pulses the reaction rate for methane formation decreases to values close to those found after LTR. Moreover, the analysis of reaction products reveals that CO is not formed and water is not detected as a reaction product during the first pulses. This stands in sharp contrast to the transient behaviour observed after LTR where little deactivation is observed: water is detected and no decline in methane formation with time is observed. The strong promotion of the activity over all the virgin catalysts after HTR is also the reason why, under pulse mode, catalyst activity is much higher than that observed under continuous steady-state conditions (compare Tables 4 and 5), although the different reaction conditions (H_2/CO_2 ratio in feed) may also contribute to the difference in activity. The following factors need to be emphasised from these experiments: (i) a marked difference exists between the catalytic behaviour measured under transient and steady-state conditions; (ii) all the catalysts, regardless of the metal employed, show an increase in activity after a high temperature reduction (if measured under transient conditions) with fast deactivation; (iii) after HTR water is retained by the catalyst at the beginning of the reaction.

A series of additional experiments in the continuous mode was carried out on Rh/CeO_2 using a diluted CO_2/H_2 mixture in He, as described in the experimental section, to obtain an accurate and continuous determination of reaction rate vs time over a virgin catalyst. In accordance with what was observed in the pulse mode, a strong and fast deactivation characterizes the behaviour of the HTR catalyst (Table 6). A similar effect is observed by using $Rh(NO_3)_3$, instead of $RhCl_3$ as the metal precursor, indicating that the precursor of the metal does not play a

TABLE 6

Catalytic Activity of Rh/CeO_2 under Continuous Conditions Using a Diluted CO_2/H_2 Mixture in He (See Experimental Section)

Red. Temp. (K)	Initial rate (μmole/$g_{cat.}$ * h)	Deactivation (%)[a]	Deposited carbon[b] (μmole/$g_{cat.}$)
473	529	49.7	157(94–63)
573	866	73.9	147(79–68)
653	1944	93.5	119(68–51)
693	3717	96.8	101(55–45)
773	7433	99.5	89(44–45)
473[c]	540	49.0	—
773[c]	5212	92.9	—

[a] Percent of deactivation after 35 minutes of reaction.

[b] Total deposited carbon determined after 35 minutes of reaction. Values obtained from the integration of the curve profile fitted with two gaussians are reported in brackets.

[c] Experiments carried out on Rh/CeO_2 prepared from $Rh(NO_3)_3$.

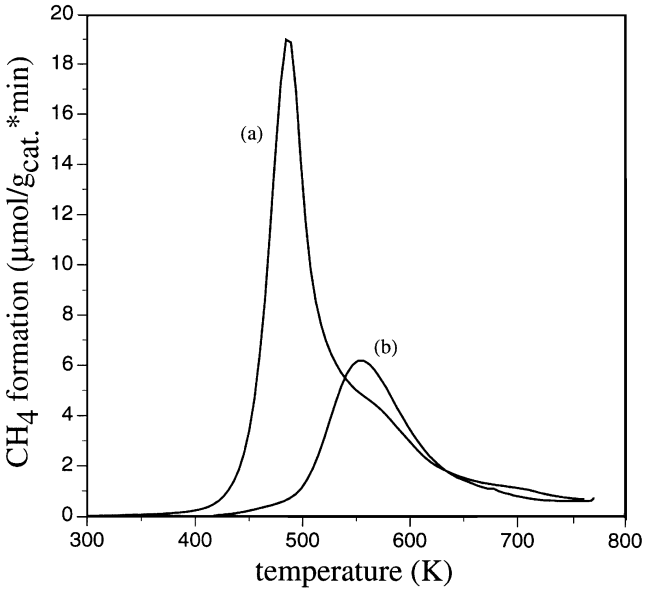

FIG. 8. Temperature-programmed methanation (TPM) of surface carbonaceous species formed after the CO_2/H_2 reaction over Rh/CeO_2 catalysts. Curve a: TPM measured after reaction. Curve b: TPM measured after reaction and treatment for 1 h under H_2 at the reaction temperature.

primary role in the determination of this transient effect. After reaching the stationary state (35 min of reaction), the H_2/CO_2/He flow was replaced with He and then with a H_2/Ar stream. The total amount of carbonaceous deposits was then determined by monitoring the CH_4 evolved during a temperature-programmed hydrogenation (Table 6). These may consist of several species containing carbon, such as carbonates, formates, and surface carbon, which can form by the interaction of CO_2 with the support under hydrogenation. A treatment under H_2/Ar of a Rh/CeO_2 catalyst, reduced at 473 K for 2 h and treated with CO_2/He at the reaction temperature, produces a quantity of CH_4 which is about 30% of the lowest value found after the catalytic reaction (32 vs 89 μmoles g^{-1}). This justifies the assumption that CH_4 evolution after the catalytic reaction is predominantly due to hydrogenation of surface carbon-containing species formed in the $CO_2 + H_2$ reaction. The results indicate that carbon formation on the catalysts during the reaction progressively decreases with increasing reduction temperature. Moreover, at least two kinds of surface carbonaceous species are present on the Rh/CeO_2 catalyst: a first species which is easily hydrogenated at temperature near 500 K and which accounts for the majority of carbon present (Fig. 8, trace a); a second species which is less reactive and much more difficult to reduce. Consistently, when the Rh/CeO_2 catalyst was kept at 463 K under hydrogen before ramping the temperature, a single peak at 560 K was observed (Fig. 8, trace b). Both species are present at higher concentrations on the LTR samples and their concentrations decrease with increasing reduction temperature. However, a deconvolution of the peak profiles by using two gaussians curves for the two carbon containing species shows that the low temperature feature is more affected by the temperature of the reduction on H_2 than the high temperature one: as the reduction temperature is increased from 473 to 773 K, the amount of CH_4 formed decreases to 47% and 71%, respectively, of the initial value (Table 6). This behaviour may suggest that the less reactive carbon-containing species are associated with surface carbonates and the decrease in their amount with increasing reaction temperature may be due to a partial loss of surface area, although the presence of a less reactive carbon species cannot be excluded. On the other hand, the more reactive carbon may be associated with surface carbon accumulated in the CO_2/H_2 reaction. Consequently these species are probably not responsible for the rapid and strong deactivation which characterizes the transient activity, although they may be responsible for the deactivation observed under steady-state conditions and which is typical of metal-supported catalysts under hydrogenation conditions (19).

DISCUSSION

The role of noble metals, particularly Rh and Pt, in the modification of the surface and catalytic properties of ceria has been the subject of several recent investigations (1–5, 7–9, 12–17). There is general agreement that a synergetic interaction between the metal and ceria is responsible for some of the interesting properties of M/CeO_2 catalysts, such as the high rate of H_2 spillover and the easy formation of oxygen vacancies in the proximity of the metal particles. In this study a systematic approach has been taken to investigate the behaviour of noble metals supported on ceria as catalysts for CO_2 activation and hydrogenation. First the interaction between H_2 and metal-supported ceria was

analyzed, followed by the investigation of the interaction between the catalysts and CO_2 following different reduction treatments; particular attention was paid to phenomena occurring under transient conditions.

Chemisorption studies are in accordance with previously published data on Rh (3, 20), Pt (21), Pd (13), and Ir (17) on ceria. The high values of H_2 uptake correlate with a high capacity of H_2 spillover from the metal to the support with the subsequent reduction of the latter. The H/M values decrease after HTR compared as compared to LTR. Such behaviour may be due to several phenomena: (i) sintering of metal particles and/or partial covering of the metal by the reduced support, although this phenomenon is likely to occur with CeO_2 only after H_2 treatment above 900 K (20); (ii) decrease in the rate of H spillover. This can be induced either by a partial dehydroxylation during the HTR (12) or by the presence of a fully reduced surface and the consequent lack of reducible surface cations which may inhibit H-spillover as observed over Pt/TiO_2 (22). Rh and Ru appear to be more efficient in promoting H_2 chemisorption even after HTR.

The result of Ru/CeO_2 is remarkable, because the use of $RuCl_3$ as a precursor generally results in low dispersions (23). These chemisorption results are also in general agreement with those observed under TPR conditions. H_2 consumed from 300 to 800 K is well above that required for reduction of the metal, indicating that the extra hydrogen is used for support reduction. This is true, providing that with the support we have used (surface area 19 $m^2\,g^{-1}$), the limitations observed by Zotin *et al.* (24) in the application of TPR to characterize high surface area ceria samples are overcome. It was recently shown that such limitations do not apply to low surface area noble-metal loaded CeO_2-based catalysts (18). Consistently, the Johnson and Mooi correlation between H_2 consumption and surface area holds for a surface area of approximately 20 $m^2\,g^{-1}$ (25). This suggests that these limitations should be absent in the present case.

All the metals show a qualitatively similar reduction behaviour; however, with RuO_2 and Rh_2O_3, a somewhat higher consumption of hydrogen for ceria reduction is observed below 500 K; this appears to be consistent with the ability of these metals to efficiently activate/adsorb H_2 even after HTR. While the presence of the metal is important at these reduction temperatures, it is less effective at high reduction temperatures (>900 K), where the reduction profile of CeO_2 is similar to that of M/CeO_2. This indicates that the metal has almost no effect on the reduction of the inner most layers of ceria.

The interaction of CO_2 with ceria and its subsequent methanation in the presence of hydrogen have been used as a probe to obtain further information on this system. Noble metals deposited on CeO_2 are active catalysts for CO_2 methanation, although their activity is lower than that observed on supports like TiO_2 and Nb_2O_5 (19, 26, 27). The order of activity for the formation of methane is $Ru > Rh \gg Ir \sim Pd > Pt$ which is qualitatively in agreement with the early work of Solymosi and Erdohely (28) on CO_2 hydrogenation over M/Al_2O_3. Although a direct comparison between these activities cannot be made due to the different reaction conditions, it is clear that, in both cases, Ru and Rh give complete selectivity to CH_4 while for Pd, Pt, and Ir, CO is also formed (Pt being the least selective). The use of CeO_2 as a support results in higher selectivities to CO with these three metals as compared to Al_2O_3, particularly in the case of Ir and Pd. Thus, a selectivity of 13% in CO was observed over Ir/Al_2O_3 (28) this increases to 93 and 97% for Ir/CeO_2 after LTR and HTR, respectively. This may suggest an active participation of the support in CO_2 dissociation. The high hydrogenation activities of Ru and Rh may account for the lack of observable CO which, being an intermediate, is rapidly hydrogenated over these metals. The reduction treatment strongly affects the interaction of CO_2 with the metal–ceria system, and the extent of CO_2 interaction with ceria is stronger when ceria has been reduced at high temperature. TPD experiments provide evidence that, after HTR, adsorbed CO_2 is reduced to CO. In all cases the amount of desorbed CO significantly increased after HTR as compared to LTR. Under these conditions, the presence of oxygen vacancies and, thus, of reduced ceria favours the reduction of CO_2 and reoxidation of the support. This is supported by running a second TPD experiment after HTR; CO formation decreased in this case, indicating that CO_2 in the first TPD run provided oxygen for a partial CeO_{2-x} oxidation, according to the following scheme:

$$M\text{-}CeO_{2-x} + xCO_2 \rightarrow M\text{-}CeO_2 + xCO.$$

Under these conditions, oxygen from CO_2 fills up the oxygen vacancies in the reduced support, thus bringing the catalyst back to a situation reminiscent of that observed after a low temperature reduction. Such a reaction is the opposite of that observed in the oxidation of CO with CeO_2, where oxygen from the support is extracted to form CO_2 (29).

Room temperature dissociation of CO_2 over a Pt/CeO_2 catalyst was proven by Daniel by monitoring the behaviour of the CO i.r. adsorption band (30). In our TPD experiments we did not detect appreciable CO evolution at room temperature. This difference may be due to the establishment of a dynamic equilibrium of dissociation and recombination of CO_2 (as reported in Ref. (30)) which may be favoured by the greater surface areas employed here. This would render the amount of CO leaving the surface by desorption negligible.

After LTR, the small amount of CO evolved in the TPD experiments indicates that CO_2 activation is inhibited under these conditions. This is probably the consequence of a limited degree of reduction of CeO_2. A quantitative

calculation as described by Johnson and Mooi (25) on the TPR reported in Fig. 3 shows that 310 μmol H_2 $g CeO_2^{-1}$ are consumed during LTR. This is approx. 2.7 times the amount required for reduction of surface CeO_2, suggesting that reduction at $T < 500$ K is mostly limited to the uppermost layers of ceria (31, 32).

The fact that pure CeO_2 shows a behaviour qualitatively similar to that observed in the presence of supported metals indicates that the promotion of the reduction of surface CeO_2 does not greatly affect the way CO_2 interacts with the support. It is only after reduction at temperatures >773 K that a relevant number of oxygen vacancies are formed, providing the driving force for CO_2 activation and reaction with ceria. Note that the H_2 consumed after HTR (Fig. 3) is 6.7 times the amount required for surface reduction. This is consistent with the mechanism proposed for ceria reduction (16, 32) which suggests that reduction takes place on the ceria support by first influencing the surface (dissociative chemisorption of H_2) and then penetrating the bulk of material leading to the creation of oxygen vacancies. The two processes and the extent to which they occur in the catalysts can be influenced by several factors. In the case of Rh, the reduction temperature, the nature of the precursor salt and the surface area of the support were found to strongly affect the degree and the nature of the reduction processes (33). According to these findings, the use of chloride as a precursor for the metal and the use of a low surface area support would increase the amount of ceria reduced by an irreversible process with the formation of oxygen vacancies. This is also supported by the results obtained with CO_2 methanation by using $Rh(NO_3)_3$ instead of $RhCl_3$ as a precursor. The reduction of the former catalyst at 773 K produces an increase of the methanation rate which is slightly lower than that observed in the latter one. This is consistent with a lower degree of irreversible reduction associated with the formation of oxygen vacancies in the case of $Rh(NO_3)_3$ (34).

A general mechanism taking these findings into account can be proposed for Rh as shown in Fig. 9. The key finding for the transient behaviour is the presence of bulk oxygen vacancies which form under high temperature reduction (H_2, $T > 773$ K) and which create the driving force required for the fast activation of CO_2. The subsequent oxidation of the support by water and/or CO_2 decomposition and the impossibility of regenerating bulk vacancies during reactions under milder conditions are the main causes of the transient behaviour and the fast deactivation which prevent the development of a full catalytic cycle. The powerful oxygen abstraction ability appears to be a general property of the reduced CeO_2 moieties. Consistently, bulk oxygen vacancies promote the NO dissociation/reduction over reduced metal-loaded catalysts containing CeO_2 (35). The main role of the noble metal (cycle 1) is that of providing reactive H-species through H_2 activation, although its role in assisting CO_2 activation under steady state conditions cannot be excluded. In addition, H-spillover from metal to ceria (Fig. 9, path (i)) or lattice oxygen migration from ceria to Rh (36) (path (ii)) contribute to the maintainance of an equilibrium concentration of active surface Ce(III) sites under the reaction conditions. The different hydrogenation capability of the catalyst after HTR and LTR is also responsible for the variation in total carbon-containing species formed during the reaction. After LTR, the carbon formed cannot be easily hydrogenated at first; some of the carbon accumulates during this reaction. A second carbon species may originate from the formation of less reactive carbon, as already reported in the cases of Rh and Ru on Al_2O_3 (19, 37), although the formation of some surface carbonates during the reaction, which may contribute to the presence of the second peak at higher temperature, cannot be excluded at this stage. Thus, while CO_2 activation could occur over the support, the successive formation, and hydrogenation of CO/surface carbonaceous species probably occurs at the M-CeO_2 interface even if long range effects cannot be excluded (36).

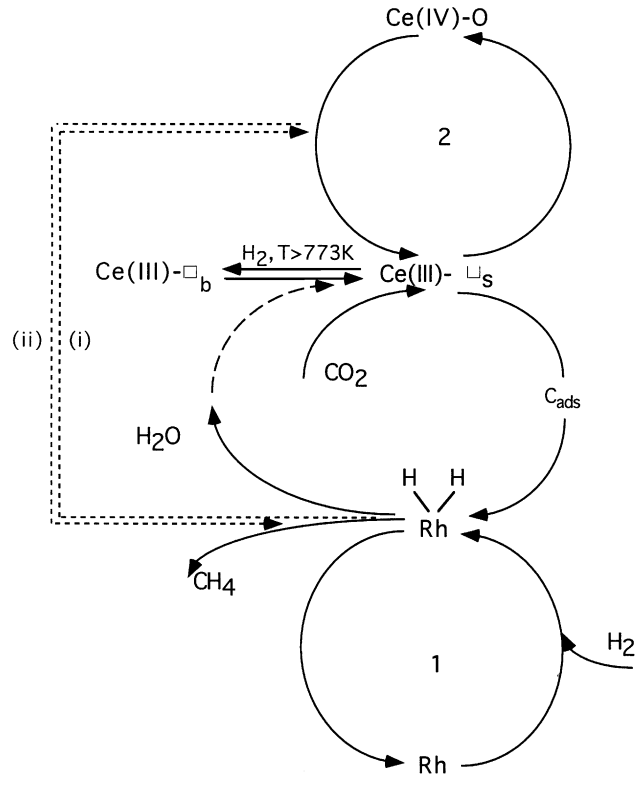

FIG. 9. Mechanistic cycle proposed for CO_2 methanation with Rh/CeO_2.

In summary, we have found that reduced ceria, as a support for noble metals, has a strong effect on CO_2 adsorption and activation. It is suggested that oxygen vacancies, and particularly those present in the bulk, are the driving force for CO_2 activation with the formation of CO and

oxidation of reduced ceria. The role of the supported metal is important in providing a source of active H-species for the hydrogenation reaction.

REFERENCES

1. Nunan, J. G., Robota, H. J., Cohn, M. J., and Bradley, S. A., *J. Catal.* **133**, 309 (1992).
2. Ranga Rao, G., Kaspar, J., Di Monte, R., Meriani, S., and Graziani, M., *Catal. Lett.* **24**, 107 (1994).
3. Trovarelli, A., Dolcetti, G., de Leitenburg, C., Kaspar, J., Finetti, P., and Santoni, A., *J. Chem. Soc. Faraday Trans.* **88**, 1311 (1992).
4. Serre, C., Garin, F., Belot, G., and Maire, G., *J. Catal.* **141**, 9 (1993); Sayle, T. X. T., Parker, S. C., and Catlow, R. C. A., *J. Chem. Soc. Chem. Commun.*, 977 (1992).
5. Trovarelli, A., de Leitenburg, C., Dolcetti, G., and Llorca, J., *J. Catal.* **151**, 111 (1995).
6. Sanchez, M. G., and Gasquez, J. L., *J. Catal.* **104**, 120 (1987).
7. Bernal, S., Calvino, J. J., Cauqui, M. A., Cifredo, G. A., Jobacho, A., and Rodriguez-lzquierdo, J. M., *Appl. Catal.* **99**, 1 (1993).
8. Datye, A. K., Kalakkad, D. S., Yao, M. H., and Smith, D. J., *J. Catal.* **155**, 148 (1995).
9. de Leitenburg, C., and Trovarelli, A., *J. Catal.* **156**, 171 (1995).
10. Kaspar, J., de Leitenburg, C., Fornasiero, P., Trovarelli, A., and Graziani, M., *J. Catal.* **146**, 136 (1994).
11. Mori, T., Masuda, H., Imai, H., Miyamoto, A., Baba, S., and Murakami, Y., *J. Phys. Chem.* **86**, 2753 (1982).
12. Bernal, S., Calvino, J. J., Cifredo, G. A., Laachir, A., Perrichon, V., and Hermann, J. M., *Langmuir* **10**, 717 (1994).
13. Bensalem, A., Bozon-Verduraz, F., and Perrichon, V., *J. Chem. Soc. Faraday Trans.* **91**, 2185 (1995).
14. Ricken, M., Nolting, J., and Riess, I., *J. Solid. State Chem.* **54**, 89 (1984).
15. Harrison, B., Diwell, A.T., and Hallet, C., *Platinum Metals Rev.* **32**, 73 (1988).
16. Yao, H. C., and Yu Yao, Y. F., *J. Catal.* **86**, 254 (1984).
17. Tournayan, L., Mancilio, N. R., and Fréty, R., *Appl. Catal.* **78**, 31 (1991).
18. Fornasiero, P., Di Monte, R., Range Rao, G., Kaspar, J., Meriani, S., Trovarelli, A., and Graziani, M., *J. Catal.* **151**, 168 (1995).
19. Solymosi, F., Erdöhelyi, A., and Bánsági, T., *J. Catal.* **68**, 371 (1981).
20. Bernal, S., Botana, F. J., Calvino, J. J., Cauqui, M. A., Cifredo, C. A., Jobacho, A., Pintado, J. M., and Rodríguez-Izquierdo, J. M., *J. Phys. Chem.* **97**, 4118 (1993).
21. Meriaudeau, P., Dutel, J. F., Dufaux, M., and Naccache, C., *Stud. Surf. Sci. Catal.* **11**, 95 (1982).
22. Huizinga, T., and Prins, R., *J. Phys. Chem.* **85**, 2156 (1981).
23. Lu, K., and Tatarchuk, B. J., *J. Catal.* **106**, 176 (1987).
24. Zotin, F. M. Z., Tournayan, L., Varloud, J., Perrichon, V., and Fréty, R., *Appl. Catal. A: Gen.* **98**, 99 (1993).
25. Johnson, M. F. L., and Mooi, J., *J. Catal.* **103**, 502 (1987); **140**, 612 (1993).
26. Trovarelli, A., Mustazza, C., Dolcetti, G., Kaspar, J., and Graziani, M., *Appl. Catal.* **65**, 129 (1990).
27. Iizuka, T., Tanaka, Y., and Tanabe, K., *J. Mol. Catal.* **17**, 381 (1982).
28. Solymosi, F., and Erdöhely, A., *J. Mol. Catal.* **8**, 471 (1980).
29. Jin, T., Okuhara, T., Mains, G. J., and White, J. M., *J. Phys. Chem.* **91**, 3310 (1987); Jin, T., Zhou, Y., Mains, G. J., and White, J. M., *J. Phys. Chem.* **91**, 5931 (1987).
30. Daniel, D. W., *J. Phys. Chem.* **92**, 3891 (1988).
31. Perrichon, V., Laachir, A., Bergeret, G., Fréty, R., Tournayan, L., and Touret, O., *J. Chem. Soc. Faraday Trans.* **90**, 773 (1994).
32. El Fallah, J., Boujana, S., Dexpert, H., Kiennemann, A., Majerus, J., Touret, O., Villain, F., and Le Normand, F., *J. Phys. Chem.* **98**, 5522 (1994).
33. Bernal, S., Calvino, J. J., Cifredo, G. A., Gatica, J. M., Omil, J. A. P., Laachir, A., and Perrichon, V., *Stud. Surf. Sci. Catal.* **96**, 419 (1995).
34. Bernal, S., Calvino, J. J., Cifredo, G. A., and Rodríguez-Izquierdo, J. M., *J. Phys. Chem.* **99**, 11794 (1995).
35. Ranga Rao, G., Fornasiero, P., Di Monte, R., Kaspar, J., Vlaic, G., Balducci, G., Meriani, S., Gubitosa, G., Cremona, A., and Graziani, M., *J. Catal.* **162**, 1 (1996).
36. Zafiris, G. S., and Gorte, J., *J. Catal.* **143**, 86 (1993).
37. Solymosi, F., Erdöhelyi, A., and Kocsis, M., *J. Chem. Soc. Faraday Trans.* **77**, 1003 (1981).